Spectroscopy and photokinetics of chromium (III) in glass

L. J. Andrews, A. Lempicki, and B. C. McCollum

Citation: J. Chem. Phys. **74**, 5526 (1981); doi: 10.1063/1.440915
View online: http://dx.doi.org/10.1063/1.440915
View Table of Contents: http://jcp.aip.org/resource/1/JCPSA6/v74/i10
Published by the AIP Publishing LLC.

Spectroscopy and photokinetics of chromium (III) in glass

L. J. Andrews, A. Lempicki, and B. C. McCollum

GTE Laboratories Incorporated, Waltham, Massachusetts 02154
(Received 9 December 1980; accepted 4 February 1981)

The optical absorption, emission, emission lifetime, and absolute quantum efficiency have been measured for chromium (III) in a wide variety of oxide and fluoride glasses. In all cases, the room temperature emission is dominated by inhomogeneously broadened $^4T_2$ fluorescence, and the relaxation of this level is shown to be primarily nonradiative. Multiphonon emission to lattice modes, concentration quenching, and quenching by hydroxyl moieties is shown not to be of significance in this relaxation at low doping levels. Instead, it is proposed that the radiationless process involves primarily local modes associated with the CrX_6 cluster and is sensitive to site symmetry.

I. INTRODUCTION

The optical properties of trivalent chromium in solids have received much attention over the years. The majority of investigations have dealt with ionic and molecular crystals which have ligand fields at the Cr(III) site sufficiently high to cause the zero phonon $^4T_2$ level to lie energetically higher than the zero phonon ^2E level. Consequently, Cr(III) emission from such solids is characterized by the relatively sharp R line transitions $^2E \rightarrow {}^4A_2$ near 700 nm as in the celebrated case of ruby, Al_2O_3 : Cr(III).[1] By contrast, the known list of materials which provide low field Cr(III) sites, here defined as those sites in which the zero phonon $^4T_2$ lies below the zero phonon ^2E, is much smaller. Included in this list are TiO_2,[2] $LiTaO_3$,[3] $LiNbO_3$,[3] $ZnWO_4$,[4] K_2NaGaF_6,[5] $Cs_2NaInCl_6$,[6,7] and the rhombic sites of MgO.[8,9] In addition, a few molecular complexes containing ligands which lie especially low in the spectrochemical series have been established to provide low field Cr(III) environments.[10–13] In all low field sites, the room temperature Cr(III) emission consists of a broad, unstructured band centered in the near infrared, which was first assigned by Parker *et al.*,[14] to the vibronically broadened $^4T_2 \rightarrow {}^4A_2$ transition. Because this transition is spin allowed, this band has been customarily labeled fluorescence. Besides these crystalline hosts, there exists a large class of little studied amorphous materials in which low field Cr(III) sites appear to be the rule rather than the exception. These are inorganic oxide and fluoride glasses, and they form the subject of the present investigation.

The optical absorption of Cr(III) in silicate glass has been known for many years and its principal features have been interpreted in terms of ligand field theory by Bamford[15] and Bates.[16] Tischer[17] was the first to systematically study the effects of compositional changes and hydrostatic pressure on Cr(III) absorption in oxide glasses, and he concluded that the Cr(III) sites are surrounded by six oxygens with approximately cubic symmetry. More recently, Brawer and White[18] have examined in detail the 650 nm band of Cr(III) in soda lime silicate glass and pointed out that the fine structure present in this band is incompatible with ligand field theory which neglects vibronic effects. Another interpretation has been given by Lempicki *et al.*,[19] who assert that the anomalous structure is due to antiresonance between sharp intraconfigurational transitions $(t_2^3 \rightarrow t_2^3)$ and a broad interconfigurational transition $(t_2^2 e \rightarrow t_2^3)$.

Broad band emission from Cr(III) in a glass was first reported by Karapetyan *et al.*,[20] and correctly assigned to $^4T_2 \rightarrow {}^4A_2$ fluorescence in a phosphate glass by Sharp *et al.*[21] Subsequent studies[22,23] by the latter group showed that Cr(III) also fluorescences in $Eu(PO_3)_3$ and a silicate glass. The only other report of Cr(III) luminescence in glass is the Brawer and White paper[18] in which Cr(III) fluorescence was used to demonstrate site inhomogeneity in soda lime silica. These authors also showed that there exists some small fraction of sites which give rise to $^2E \rightarrow {}^4A_2$ phosphorescence, that is, the range of available ligand fields span both high and low field cases.

Clearly, our knowledge of the luminescence of Cr(III) in glass is fragmentary and our present purpose is to characterize this emission in a wide variety of glasses representative of many major glass types. We have placed particular emphasis on the dynamics and efficiencies of the $^4T_2 \rightarrow {}^4A_2$ relaxation processes and their dependence on glass composition. That this is an especially neglected area is apparent when one considers that a direct measure of the $^4T_2 \rightarrow {}^4A_2$ radiative efficiency has not been previously reported for any Cr(III) low field material. Finally, specific consideration has been given to multiphonon relaxation, concentration quenching and quenching by hydroxyl moieties as possible nonradiative relaxation mechanisms for Cr(III) in glass.

II. MATERIALS AND TECHNIQUES

A. Glass composition and preparation

The 20–25 g samples were prepared using 4–9 s components where possible. The phosporic acid component of phosphates was electronic grade. The formulation of the commercial $Al(PO_3)_3$ used in the preparation of several glasses was probably inexact because of the difficulty of the control of P_2O_5 loss during its preparation. All samples were melted in platinum crucibles to minimize contamination with the exception of phosphate glasses which were prepared in alumina crucibles.

The materials were melted in a silicon carbide element muffle furnace rated at 1600 °C, which was con-

 0021-9606/81/105526-13$01.00

TABLE I. Glass compositions and melt temperatures.

Type	Composition (mol%)	Melt temperature (°C)
Aluminum phosphate	Al_2O_3-28.9, $P_2O_5^*$-71.1	1450
Zinc aluminum phosphate	$Al(PO_3)_3$-73.4, ZnO-26.5	1000
Calcium phosphate	$CaCO_3$-33.3, P_2O_5-67.7	1000
Sodium phosphate	Na_2CO_3-33.3, P_2O_5-67.7	1000
Fluorophosphate 1 O/F = 2.3	$Al(PO_3)_3$-23.7, NaF-61.3, CaF_2-15.0	850
Fluorophosphate 2 O/F = 0.22	$Al(PO_3)_3$-5.0, AlF_3-24.96 NaF-5.0, LiF-5.0, MgF_2-10.0 CaF_2-30.0, SrF_2-10.0, BaF_2-10.0	850
Fluorophosphate 3 O/F = 0.10	$Al(PO_3)_3$-2.4, AlF_3-27.6, NaF-15.0 MgF_2-13.0, BaF_2-4.6, CaF_2-31.0 SrF_2-6.4	850
Lithium borate	B_2O_3-66.7, Li_2CO_3-32.3, As_2O_3-1.0	1100
Lithium aluminum borate	B_2O_3-65.0, Li_2CO_3-20.0, Al_2O_3-13.9 As_2O_3-1.0	1100
Soda lime silicate	SiO_2-73.0, Na_2CO_3-14.0, $CaCO_3$-13.0	1550
Lithium lime silicate 1	SiO_2-58.9, Li_2CO_3-27.5, $CaCO_3$-10.0 Al_2O_3-2.5, As_2O_3-1.0	1550
Lithium lime silicate 2	SiO_2-60.0, Li_2CO_3-27.5, $CaCO_3$-10.0 Al_2O_3-2.5	
Borosilicate	SiO_2-65.0, Na_2CO_3-20.0 B_2O_3-15.0	1400
Tellurite	TeO_2-78.5, Na_2CO_3-15.0, K_2O-5.0 As_2O_3-1.0	800
Phosphotungstate	WO_3-48.3, Na_2HPO_4-51.6, Cr_2O_3-0.1	1000
Fluorozirconate	ZrF_4-57.5, BaF_2-33.75, ThF_4-8.75	•••

*P_2O_5 added as H_3PO_4

structed to allow the use of controlled furnace atmospheres. In order to minimize Cr(VI) contamination, the samples were initially heated in a nitrogen atmosphere established by flushing the furnace overnight. A switchover was made to argon at about 1000 °C in order to preserve the SiC elements. In some glasses, As_2O_3 was also added to reduce Cr(VI). The molten glasses were poured into preheated graphite molds after 1 to 2 h at temperature in the muffle furnace. The samples were then annealed at an appropriate temperature to relieve strains and then cooled to room temperature. The phosphates required removal of water from the samples by heating to 700° over a 16 to 18 h programmed heating schedule. These were then transferred to the muffle furnace and treated as indicated for other glasses. Samples fabricated for spectroscopic and quantum yield measurements were cut and polished into $2\times5\times5$ or $2\times10\times10$ mm pieces. The compositions given in Table I are for the components added except for some of the phosphates in which P_2O_5 was added as H_3PO_4. For the high melting aluminum phosphate, the final composition is given. This will vary somewhat from sample to sample; for example, due to P_2O_5 volatilization, the initial Al_2O_3 content for this glass was 19.0 mol percent and the final was 28.9 mol%.

The soda lime silicate sample prepared to minimize the hydroxyl was prepared as above with dried starting materials. The furnace temperature was lowered several hundred degrees to increase the melt viscosity and then the sample was quickly transferred to the annealing furnace without pouring in order to minimize the absorption of moisture from the air. Portions of the sample were dried under dynamic vacuum at 710 °C. Other parts were ground to a powder, mixed with either NaCl or NaF, dried under dynamic vacuum at 200 °C, and then processed as noted to minimize contamination. Refusion with NaF was found to be the most effective means of reducing the hydroxyl content.

B. Experimental techniques

Fluorescence lifetime measurements of Cr(III) doped glasses were made using a Rhodamine-6G dye laser (0.1 nm resolution, 5 ns pulse duration) tuned near 585 nm

for excitation, an 800 nm broad band interference filter to isolate emission, and an RCA 4832 GaAs photomultiplier for detection. Time-resolved spectra were recorded with a 0.5 m Jarrell-Ash spectrometer, a PAR model 162 box car integrator, and the 4832 photomultiplier. Steady state emission spectra were recorded using HeNe laser excitation, the 0.5 m Jarrell-Ash, and a Varian VPM 159 A.12D photomultiplier. The steady state spectra were corrected for wavelength variations in the system response by calibrating the spectrometer-photomultiplier unit with a standard 1 kW tungsten halogen lamp. The Sylvania DXW working lamp was itself calibrated against an NBS standard lamp.

Absorption spectra were measured using either a Cary 17 or 118 spectrophotometer, except for the liquid He spectrum which was measured at a low temperature, high resolution facility at MIT. The room temperature extinction coefficients (ϵ, 1 mol^{-1} cm^{-1}) of several glasses were calculated from the absorption data and the glass density. The density was measured by weighing cut and polished samples of accurately known dimensions. The Cr(III) content was assumed equal to twice the amount of Cr_2O_3 used in the sample preparation since the absorption spectra showed only Cr(III) present in the glasses. An oxidation to Cr(VI) would have easily been detected by the intense Cr(VI) charge transfer band at 366 nm. The densities and ϵ values for the first broad absorption band ($^4T_2 \rightarrow {}^4A_2$) are given below.

Glass	Density ($g\,cm^{-3}$)	ϵ (1 mol^{-1} cm^{-1})
Fluorophosphate 1	2.71	19.1
Soda lime silicate	2.48	21.5
Lithium aluminum borate	2.17	26.3

These values are accurate to ±10% and are in agreement with Tischer's[17] results for similar compositions.

Quantum yield measurements were done using an integrating sphere with diameter 33.8 cm. The entrance port for the HeNe excitation beam was 3 mm and the photomultiplier viewing port was 1 cm. The field of view for the photomultiplier was aligned and baffled so as to avoid direct illumination from a source at the center of the sphere. Glass samples cut and polished into 5×5×2 mm sizes were cemented by a corner onto 5 mm diameter rods which could be used to accurately and reproducibly position the sample in the center of the sphere. The sample was aligned so that the excitation beam was approximately normally incident to a 5 ×5 mm surface. All interior surfaces of the sphere including the sample rods were coated with Eastman White Reflectance Paint (#6080) applied according to the manufacturer's instructions. The HeNe excitation was passed through a narrow band 632.8 nm interference filter to remove continuum radiation and attenuated to insure that the RCA 4832 photomultiplier was operated in a linear response range (<30 nA). The quantum yield measurement was performed by sequentially placing an undoped blank and doped samples into the excitation beam. Excitation and fluorescence radiation were isolated using a second 632.8 nm interference filter and a Schott RG665 cutoff filter, respectively. The optical transmissions of these filters were measured on two spectrophotometers which gave identical results. When measuring the transmission of the HeNe filter, care was taken to calibrate the spectrometer wavelength by using the 656.1 nm D_2 line. Since the useful sensitivity of the GaAs photomultiplier extends only to 900 nm, its response had to be convoluted with the corrected glass emission spectrum in order to calculate the quantum yield. The 4832 photomultiplier response (amp/photon s^{-1}) was measured by comparison with an Eppley multijunction thermopile using a 15 W tungsten lamp focused onto a 0.25 m Jarrell-Ash spectrometer as a source. To compensate for the vastly different photomultiplier and thermopile sensitivities, the spectrometer slits were made narrow and the lamp lens defocused for the photomultiplier measurement.

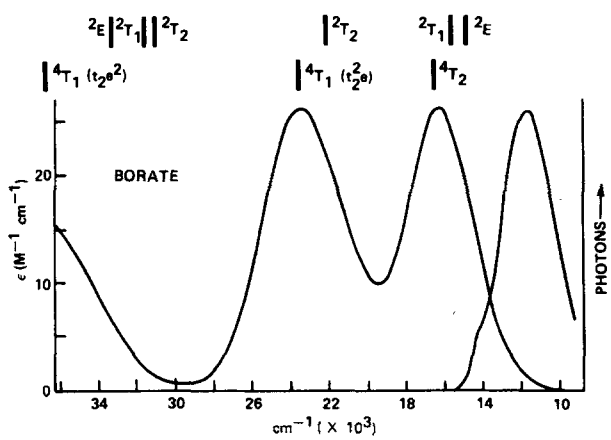

FIG. 1. Absorption and emission spectrum of Cr(III) in lithium aluminum borate glass. Ligand field state energies are shown as bars above the spectrum. The higher set of doublets are derived from the t_2e^2 configuration. The corrected room temperature fluorescence spectrum shown on the right was measured from a sample containing 0.02 mol% Cr_2O_3.

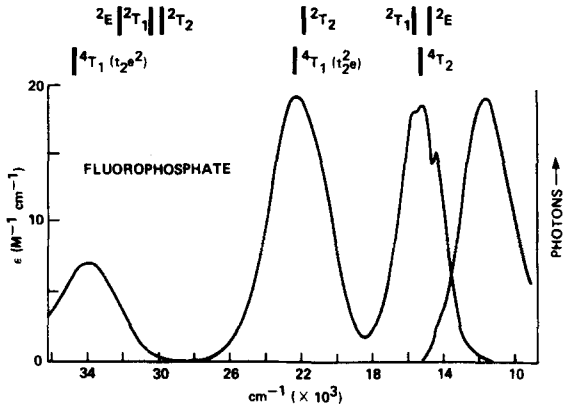

FIG. 2. Absorption and emission spectrum of Cr(III) in fluorophosphate 1 glass (O/F = 2.3).

III. RESULTS

A. Absorption and emission spectra

The optical absorption and emission spectra of Cr_2O_3 or CrF_3 dissolved in lithium aluminum borate, fluorophosphate and aluminum phosphate glasses are shown in Figs. 1–3. These spectra were chosen as repre-

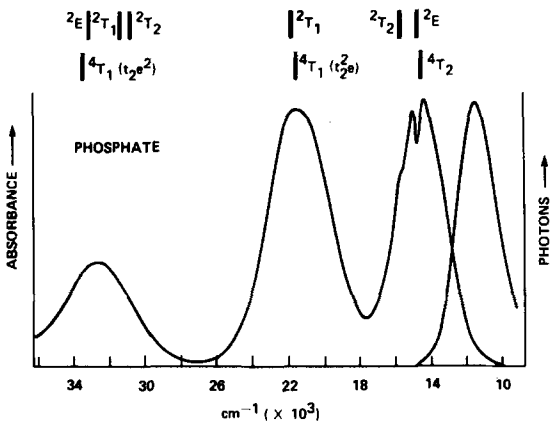

FIG. 3. Absorption and emission spectrum of Cr(III) in aluminum phosphate glass.

sentative of the range of behavior found for the glasses studied here. The absorption spectra are similar to those previously reported for Cr(III) in glass[17] and the emission spectra confirm earlier work which indicated that the Cr(III) luminescence in glass is a broad, Stokes' shifted band centered in the near infrared.[18,20,21] All bands in absorption are explicable in terms of forbidden d–d ligand field transitions associated with d^3 Cr(III). In particular, there is a complete absence of the strong Cr(VI) charge transfer transition located near 366 nm which can completely obscure higher energy ligand field bands in partially oxidized glasses.[24]

The principal features in absorption are three bands which are easily identified as the vibronically broadened transitions $^4T_2 - {}^4A_2$; $^4T_1(t_2^2e) - {}^4A_2$, and $^4T_1(t_2e^2) - {}^4A_2$, in order of increasing energy. Since no splitting is apparent in these bands, they are consistent with a Cr(III) site surrounded by a regular octahedron of nearest neighbor ions as pointed out by others.[15,18] This is true even of fluorophosphate glass shown in Fig. 2 which has an atomic oxygen/fluorine ratio of 2.3. In this case it is highly likely that an average, both oxide and fluoride ions are present in the Cr(III) coordination sphere, which should reduce the Cr(III) site symmetry. Nevertheless, the absorption is very similar to a fluorophosphate glass which has an oxygen/fluorine ratio of 0.10 or to glasses in which only coordination to oxygen is possible. This apparent simplicity in the Cr(III) environment is a reflection of the inhomogeneously broadened nature of the bands. As will be discussed in detail in the next section, there is ample evidence that Cr(III) in glass occupies a continuous range of sites so that splittings due to low site symmetry tend to be obscured by the superposition of many single site spectra. Variations in the bandwidth among the glasses shown in Figs. 1–3 are attributable to differences in this inhomogeneous broadening. The width of transitions increases along the series phosphate < fluorophosphate ~ silicate < tellurite ~ fluorozirconate ~ phosphotungstate < borate.

In addition to broad features, the absorption spectra show fine structure in the vicinity of the $^4T_2 - {}^4A_2$ band which is due to the transitions $^2E - {}^4A_2$ and $^2T_1 - {}^4A_2$. The disagreement concerning the detailed assignment of this structure has been discussed at length by Brawer and White,[18] and we favor a Fano antiresonance interpretation.[19] In this scheme, the sharp t_2^3 intraconfigurational transitions undergo destructive interference with the $^4T_2$ vibronic quasicontinuum causing a cancellation of absorptive intensity. The best example of this is the aluminum phosphate spectrum (Fig. 3) in which the structure on the $^4T_2$ band is interpreted as two antiresonant notches associated with the two lowest energy doublets rather than three sharp features of unsettled origin perched on a broad interfigurational transition. This has a practical consequence of assigning the $^2T_1 - {}^4A_2$ and $^2E - {}^4A_2$ transition energies to minima (approximately) rather than to spectral peaks. Full details concerning this effect have been presented elsewhere.[19,25]

Table II contains a summary of absorption spectroscopic data for Cr(III) in a wide variety of glass hosts. These data were used to calculate strong field parameters using the Tanabe–Sugano[26] matrices in the following manner. D_q and B were fixed by the $^4T_2$ and $^4T_1(t_2^2e)$ peak positions, respectively, then C was varied to provide the best fit to the ^2E and $^2T_1$ transition energies. The resulting state energies for the glasses in Figs. 1–3 are shown as vertical bars above the spectra.

From these data, it is clear that the value for D_q in glass is determined primarily by the network former and increases along the series phosphate < silicate ~ fluorophosphate < borate, which is in agreement with earlier work.[17] Within each of these classifications smaller variations in D_q accompany changes in the network modifier ion. It should be stressed here that the ligand field parameters listed in Table II are average or most probable values for each glass, and that a more accurate model of the glass environment would recognize that a distribution of values actually exists.

In Table III there is a summary of the emission spectroscopic data for the glasses listed in Table II. In all cases, the room temperature emission is dominated by a broadband located in the near infrared which forms an approximate mirror image with the $^4T_2 - {}^4A_2$ transition in absorption. There is no doubt that this band is the corresponding $^4T_2 - {}^4A_2$ transition in emission. It is clear, then, that the majority of Cr(III) sites in glass are low field such that the $^4T_2$ lies below the ^2E level in the thermally relaxed excited state. In many glasses, this emission is accompanied by a small shoulder on the short wavelength edge which, as pointed out by Brawer and White,[18] is associated with the $^2E - {}^4A_2$ fine structure in absorption. This feature is particularly evident at 14 600 cm^{-1} in the emission spectrum of soda lime silicate glass at liquid helium temperature (Fig. 4), and is reasonably assigned to the R line emission of Cr(III) in high field sites. Some effort was expended in formulating borate glasses to increase the proportion of high field sites by substituting Na_2O or K_2O for Li_2O and by varying the proportion of Al_2O_3 to B_2O_3. Although some variation in the fraction of R line to total luminescence could be effected, the dominant emission at ambient temperature always remained $^4T_2 - {}^4A_2$.

TABLE II. Summary of spectroscopic data for Cr (III) absorption in glass.[a]

Glass	$^2E \leftarrow {}^4A_2$	$^2T_1$	$^4T_2$	$^4T_1(t_2^2 e)$	$^4T_1(t_2 e^2)$
Aluminum phosphate	14 760	15 630	14 500	21 500	32 510
	$D_q = 1450$	$B = 761$	$C/B = 4.08$		
Zinc aluminum phosphate	14 770	15 650	14 600	21 550	33 490
	$D_q = 1460$	$B = 749$	$C/B = 4.18$		
Calcium phosphate	14 770	15 630	14 750	21 740	33 560
	$D_q = 1477$	$B = 752$	$C/B = 4.15$		
Sodium phosphate	14 750	15 550	15 080	22 080	...
	$D_q = 1508$	$B = 745$	$C/B = 4.19$		
Fluorophosphate 1 O/F = 2.3	14 760	15 580	15 270	22 360	33 840
	$D_q = 1527$	$B = 754$	$C/B = 4.11$		
Fluorophosphate 2 O/F = 0.22	14 880	15 820	15 460	22 780	34 600
	$D_q = 1546$	$B = 787$	$C/B = 3.92$		
Fluorophosphate 3 O/F = 0.10	15 040	15 930	15 520	22 750	...
	$D_q = 1552$	$B = 770$	$C/B = 4.11$		
Soda lime silicate	14 760	15 560	15 200	22 250	...
	$D_q = 1520$	$B = 750$	$C/B = 4.15$		
Lithium lime silicate 1	14 710	15 500	15 480	22 570	...
	$D_q = 1548$	$B = 749$	$C/B = 4.12$		
Borosilicate	14 730	15 550	15 220	...	...
	$D_q = 1522$				
Lithium borate	14 270	15 170	15 530	23 200	...
	$D_q = 1553$	$B = 845$	$C/B = 3.24$		
Lithium aluminum borate	14 710	15 600	16 420	23 530	...
	$D_q = 1642$	$B = 732$	$C/B = 4.29$		
Tellurite	14 170	14 920	15 440	21 660	...
	$D_q = 1544$	$B = 623$	$C/B = 5.13$		
Phosphotungstate	14 390	15 130	15 110	22 170	...
	$D_q = 1511$	$B = 754$	$C/B = 3.94$		
Fluorozirconate	15 430	16 210	14 970	22 370	...
	$D_q = 1497$	$B = 816$	$C/B = 3.89$		

[a]Band positions are in units of cm^{-1}.

B. Inhomogeneous broadening

The decay kinetics of the broad infrared emission of Cr(III) doped soda lime silicate glass are complex. The decay is highly nonexponential and varies within the luminescence band such that it accelerates as the emission wavelength becomes longer. Accordingly, the band undergoes an easily detected blue shift with time. This complex behavior persists even in highly dilute samples (0.002 mol% Cr_2O_3) so that complications due to chromium–chromium interactions can be safely neglected in its interpretation (see Sec. III D). On the other hand, the data appear consistent with a model which has isolated Cr(III) occupying a variety of sites characterized by different ligand fields and therefore possessing different spectra, and which are also distinguished by wide variations in relaxation rate. In the case of silicate glass, it is the higher field sites which have the slower relaxation.

Further evidence for site multiplicity can be simply obtained by measuring the absorption-emission overlap of samples cooled to liquid-helium temperature. At this low temperature the contribution of hot bands to the overall spectra is almost negligible, and the coincidence of band origins should be observable. As shown in Fig. 4, the spectra for Cr(III) in soda lime silicate glass do not have any such simplicity but rather overlap by more than 2000 cm^{-1}. This overlap can be attributed to a multiplicity of sites which vary continuously in li-

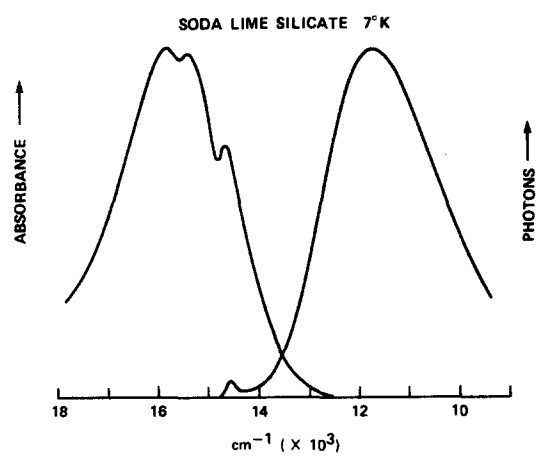

FIG. 4. Liquid He absorption and uncorrected emission spectra of Cr (III) in soda lime silicate glass.

TABLE III. Summary of spectroscopic data for Cr(III) fluorescence in glass.

Glass	$^4T_2 \rightarrow {}^4A_2$ (cm^{-1})	$\Delta\nu$ (cm^{-1})[a]	$\bar{\tau}$ (μs)[b]	ϕ[c]
Aluminum phosphate	11 590	2580	30	0.10
Zinc aluminum phosphate	11 520	2510	20	•••
Calcium phosphate	11 720	2400	•••	•••
Sodium phosphate	11 900	2490	18	0.06
Fluorophosphate 1 O/F = 2.3	12 000	2580	23	0.10
Fluorophosphate 2 O/F = 0.22	11 860	2720	37	0.02
Fluorophosphate 3 O/F = 0.1	11 950	2850	37	0.04
Soda lime silicate	11 970	2890	34	0.08
Lithium lime silicate 1	12 110	2910	30	0.17
Borosilicate	12 120	2720	34	0.08
Lithium borate	12 390	3110	10	•••
Lithium aluminum borate	12 250	3220	20	0.01
Tellurite	11 090	3260	5	0.01
Phosphotungstate	11 780	2830	6	0.005
Fluorozirconate	•••	•••	•••	0.00

[a]Bandwidth at half-height.
[b]See Sec. III B for definition of the average lifetime $\bar{\tau}$.
[c] ϕ is the absolute quantum efficiency defined photons emitted/photons absorbed. Those glasses for which ϕ is not reported are particularly hydroscopic.

gand field parameters and which must to some extent inhomogeneously broaden the band. From a comparison of the overall bandwidth to the extent of overlap in Fig. 4, it also follows that the inhomogeneous contribution to the $^4T_2 \rightarrow {}^4A_2$ bandwidth must be minor. This is in qualitative agreement with the time resolved spectral measurements which show that the blue shift amounts to at most 10% of the total emission bandwidth. The dominant broadening mechanism in glass, as in other solids, can be attributed to strong phonon coupling of the electronic transition which is expected for interconfigurational d–d transitions such as $t_2^2 e \rightarrow t_2^3$.

In potassium aluminum borate glass, Cr(III) site heterogeneity leads to pronounced time-resolved spectral changes as shown in Fig. 5. Such large changes can be understood when one recognizes that borate glasses provide the highest average ligand field of any glass so far investigated. This leads to an appreciable population of sites at the high end of the distribution which cause the $^4T_2$ and ^2E levels to invert so that in the absence of energy transfer among Cr(III) ions, both the sharp intraconfigurational $^2E \rightarrow {}^4A_2$ transition and the broad $^4T_2 \rightarrow {}^4A_2$ band can appear in emission. Figure 5 shows that not only are both types of emission present in borate glass, but that they have very different decay characteristics. The relatively sharp R line near 689 nm decays approximately exponentially with a 1 ms lifetime at helium temperature. This is about a factor of 10 slower than the average $^4T_2$ lifetime at the same temperature. Similar results have been found for other glasses. Figure 4 shows that the R line appears weakly in the steady state emission of silicate glass even though the average value for D_q is ~100 cm^{-1} lower than for the borate. Pulsed experiments are more difficult for the silicate glass since the fraction of high field sites is lower, but decay measurements at helium temperature

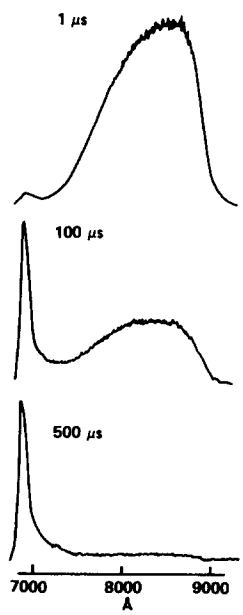

FIG. 5. Time resolved liquid He emission spectra of Cr (III) in potassium aluminum borate glass. The RCA 4832 GaAs PM truncates the $^4T_2$ fluorescence at ≅ 900 nm. The peak intensities of these spectra were arbitrarily normalized to approximately equal values.

show that the R line lifetime is much longer than the broadband emission. Even in aluminum phosphate glass which has an average D_q 200 cm^{-1} lower than the borate, an extremely weak R line could be detected at helium temperature. In this case pulsed experiments were not attempted.

The corollary to emission experiments in demonstrating inhomogeneous broadening is to investigate the effects of variations in excitation wavelength. Brawer and White[18] showed that the position of the $^4T_2 \rightarrow {}^4A_2$ fluorescence of Cr(III) in silicate glass was dependent on which argon ion laser line was used for excitation, and they invoked site heterogeneity to explain this result. We have not extensively investigated this point, but it was shown that for borate, silicate and phosphate glasses the ratio of R line to broadband emission is a function of excitation wavelength when the $^4T_2 \rightarrow {}^4A_2$ band is pumped. The ratio varies in the expected direction, that is, as the excitation was tuned from the red to the blue edge of the band the relative amount of R line intensity increases because a larger fraction of high field sites are selected. In fact, for the aluminum phosphate glass, it was only possible to detect the R line when the blue edge of the $^4T_2 \rightarrow {}^4A_2$ band was pumped.

As mentioned earlier, the $^4T_2 \rightarrow {}^4A_2$ decay is highly nonexponential in glass. Nevertheless, it is useful to have some measure of the lifetime to facilitate comparisons among glasses. For this reason we define an average lifetime $\bar{\tau}$ as follows:

$$\bar{\tau} = \int_0^\infty tI(t)dt \Big/ \int_0^\infty I(t)\,dt \ ,$$

where $I(t)$ is the experimental decay curve. Ambient temperature values for $\bar{\tau}$ range from 6–40 μs and are listed in Table III. Since concentration quenching manifests itself as accelerated decay rates, these values refer to the dilute limit where $\bar{\tau}$ is independent of Cr(III) doping level. All values are for excitation at 585 nm although we found $\bar{\tau}$ to be insensitive to variations in excitation wavelength throughout the Rhodamine-6G dye laser tuning range. Finally, R line contribution to this measurement was excluded by isolating the $^4T_2 \rightarrow {}^4A_2$ emission with an 800 nm interference filter.

C. $^4T_2 \rightarrow {}^4A_2$ quantum yield

One of the goals of this research was to determine the absolute quantum yield (photons emitted/photons absorbed) of the Cr(III) infrared $^4T_2$ emission and its dependence on glass composition. A convenient optical method for doing this uses an integrating sphere, and this method was adopted here. The advantage of the integrating sphere over other optical techniques is that the detector response depends only on the total emission intensity I_0 (photons/s) of a radiant source located at the center of the sphere and is completely insensitive to the unavoidable spatial anisotropies associated with the source emission. To understand this, one need only consider that the surface of a perfect integrating sphere is coated with a diffusive matte finish so that light striking any portion of the surface obeys the $\cos\theta$ reflectance law, thereby uniformly illuminating every other portion of the sphere. In practice this performance can be very nearly achieved. For proper operation it is necessary that the fractional absorptivity α of the surface be small, so that little light is lost on the first reflection, and that the detector not view the source directly. These are two easily fulfilled requirements. A useful discussion of the integrating sphere method for quantum yield determinations has been given by Forster and Livingston.[27]

It has been shown[28] that the indirect illumination I (that light which has suffered at least one reflection) striking a detector which views an arbitrary portion of the sphere's inner surface is related to the total intensity I_0 of a source located at the center of the sphere as follows:

$$I = cI_0G(1/\alpha - 1) \cong cI_0G/\alpha \ , \quad \alpha \ll 1 \ , \tag{1}$$

where c is a constant dependent on the detector field of view and G is the fractional transmission of any filters used to isolate the source luminescence. Since the detector is a photomultiplier, it is convenient to explicitly relate intensity to anode current i using the photomultiplier quantum efficiency S (amp/photon s^{-1})

$$\begin{aligned} i &= SI \cong cSI_0G/\alpha \ , \\ I_0 &\cong \alpha i/cSG \ . \end{aligned} \tag{2}$$

Two quantities are needed to compute the quantum yield ϕ, the absorbed excitation intensity A and the luminescence intensity L.

Since the excitation beam transmitted by the sample is equivalent to a highly anisotropic radiant source, A is given by

$$\begin{aligned} A &= I_0(\text{blank}) - I_0(\text{sample}) \ , \\ &\cong \alpha_A \Delta i_A / cS_A G_A \ , \end{aligned} \tag{3}$$

where the subscript refers to the values of the constants at the wavelength of excitation and it is assumed that the filter G_A is opaque to luminescence. Similarly for L

$$\begin{aligned} L &= I_0(\text{sample}) - I_0(\text{blank}) \\ &\cong \alpha_L \Delta i_L / cS_L G_L \ . \end{aligned} \tag{4}$$

Then ϕ is given by

$$\phi = L/A \cong \alpha_L \Delta i_L S_A G_A / \alpha_A \Delta i_A S_L G_L \ . \tag{5}$$

Recognizing that the excitation is monochromatic and that emission occurs over a band, Eq. (5) is rewritten as

$$\begin{aligned} \phi &\cong \Delta i_L G_A / \Delta i_A G_L \bar{S}_L \ , \\ \bar{S}_L &= \int_0^\infty S(\lambda)L(\lambda)d\lambda \Big/ \int_0^\infty L(\lambda)d\lambda \ , \end{aligned} \tag{6}$$

where the ratio α_L/α_A is assumed unity (see below) and S_L is replaced by $\bar{S}_L$ which is the average value of $S(\lambda)$ over the luminescence band $L(\lambda)$. Since it is only necessary that $S(\lambda)$ represent the relative photomultiplier quantum efficiency, $S(\lambda)$ can be normalized to its value at 632.8 nm which means S_A is unity in Eq. (6). The

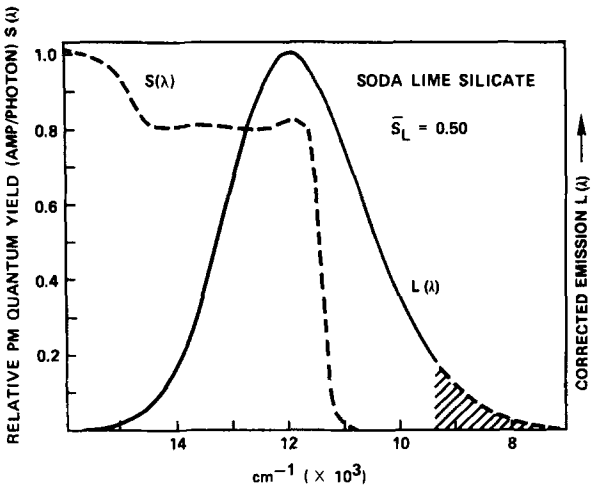

FIG. 6. Plots of $L(\lambda)$ for soda lime silicate glass and $S(\lambda)$ illustrating the calculation of $\bar{S}_L$. $L(\lambda)$ is the corrected room temperature fluorescence spectrum and $S(\lambda)$ is the relative quantum efficiency of the RCA 4832 GaAs photomultiplier.

functions $S(\lambda)$ and $L(\lambda)$ are shown in Fig. 6 for soda lime silicate glass, and for this case $\bar{S}_L$ is calculated to be 0.50. Notice that $L(\lambda)$ is the corrected emission spectrum to which has been added a long wavelength tail which was calculated assuming that the red edge emission intensity drops off as a Gaussian. The area under this unobserved emission is denoted by cross hatches in Fig. 6. For the glasses studied here, $\bar{S}_L$ varies between 0.4 and 0.6, the upper limit represented by lithium aluminum borate and the lower limit by aluminum phosphate.

It is worthwhile to emphasize that two correction procedures must be used to determine $\bar{S}_L$. First, $S(\lambda)$ is obtained by using a thermopile to calibrate the wavelength variation of the photomultiplier quantum efficiency, while taking care to note that a thermopile has a flat energy, not photon, response. Second, the glass emission spectrum must be recorded by a spectrometer-photomultiplier unit which has been calibrated with a standard lamp. Both of these procedures conspire to make $\bar{S}_L$ probably the largest source of systematic error in the calculation of ϕ. This is the penalty to be paid for the sensitivity and convenience of using a photomultiplier rather than a thermopile detector as has been done in the past.[27] Even so, $\bar{S}_L$ should not introduce objectionably large uncertainty in ϕ since S and L appear as integrated quantities in the final expression.

It has been assumed in Eq. (5) that the ratio α_L/α_A is unity, that is, the interior surface of the sphere has a flat absorption coefficient between the wavelength limits 632.8 and 900 nm. The material used to prepare this surface was a commercial reflectance paint which consists of barium sulfate in a binder-solvent suspension. When properly applied, this paint has been found[29] to have low absorptivity and good diffuse reflection qualities for radiation in the visible and near infrared. In particular, its reflectivity was measured[29] to be flat in the wavelength region of interest here, and this was assumed to be true for the sphere inner surface.

In using an integrating sphere, attention must be given to errors caused by the absorption of luminescence by unexcited centers when the quantum efficiency of the centers is low and the absorption-emission spectral overlap is appreciable, as it is for the Cr(III) doped glasses shown in Figs. 1–3. Errors arise in two ways. First, multiple reflections within the sphere make it possible that the luminescence passes repeatedly through the sample and is lost through absorption. Second, transmission of the luminescence to a sample surface subsequent to excitation can lead to significant self-absorption error if the doping level is high. Experimentally, the usual practice is to minimize both sources of error with small sample volumes and low ion doping levels. In our apparatus, the ratio of sphere volume to sample volume is 4×10^5. Also, HeNe laser excitation coincides closely with the $^4T_2 - {}^4A_2$ band maximum so that Cr(III) concentrations near 0.03 mol% are practical for yield measurements with reasonable precision. Nevertheless, we do find even at the lowest practical doping levels that a fourfold increase in sample volume (from $5\times5\times2$ mm to $10\times10\times2$ mm) results in a 10% reduction in the measured yield, a decrease which is just detectable within the precision of the technique. We make a correction for this small self-absorption error in the following manner.

The quantum efficiency is proportional to the integrated luminescence decay curve as follows:

$$\phi = \tau_R^{-1} \int_0^\infty I(t)\,dt\ , \tag{7}$$

where τ_R is the radiative lifetime and $I(t)$ is the experimental emission decay function. This relation was used to construct Cr(III) concentration quenching profiles by measuring the areas under decay curves which have a normalized initial intensity. The only assumptions inherent in Eq. (7) are the reasonable ones that τ_R is independent of doping level and the lifetime lengthening due to luminescence trapping is negligible because of the low probability of consecutive emission events. From this experimental curve (shown in Fig. 7 for

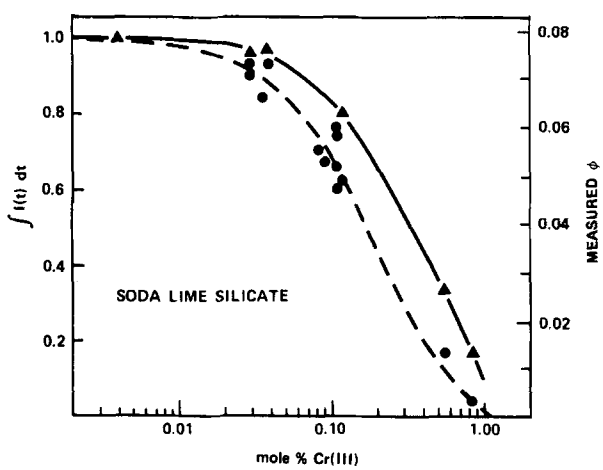

FIG. 7. Plot of the integrated experimental fluorescence decay curves (triangle) of Cr(III) in soda lime silicate glass as a function of Cr (III) concentration is shown together with measured quantum yields (circles). The dashed curve is a calculated correction for self-adsorption loss. See text for details.

soda lime silicate), which depends only on Cr(III)–Cr(III) interaction and not self-absorption, a calculated dependence on self-absorption can be derived by assuming an effective luminescence path length within the sample and using the average extinction coefficient in the absorption-emission overlap region ($4\,\ell\ \text{mol}^{-1}\ \text{cm}^{-1}$ for soda lime silicate). This curve calculated for $l = 5$ mm is shown in Fig. 7. The integration sphere ϕ values for soda lime silicate samples at a variety of Cr(III) doping levels (all samples $5\times5\times2$ mm) are compared with this calculated curve by constraining the average of the most lightly doped samples [0.034 mol% Cr(III) and $\phi = 0.071$] to lie on the calculated curve. The resulting fit to the remaining samples shown in Fig. 7 is satisfactory. Similar treatments using $l = 2$ and 10 mm resulted in obviously unacceptable fits to the integration sphere data. In this way we estimate that ϕ for soda lime silicate at doping levels of 0.03 to 0.04 mol% is reduced 5% due to self-absorption and 5% due Cr(III) concentration quenching. The ϕ value listed in Table II has been corrected accordingly. Since the extent of absorption-emission overlap is similar in all the glasses and the Cr(III) concentration quenching profiles are also quite similar (see Sec. III D) the same correction has been applied to all the ϕ values reported in Table III.

The absolute quantum efficiencies for Cr(III) $^4T_2 \rightarrow {}^4A_2$ emission in the silicate, phosphate, and fluorophosphate glasses studied here are all close to 0.1. The highest value is for lithium lime silicate at 0.17. The borate glasses have efficiencies about tenfold lower, and the tellurite and phosphotungstate glasses are similar or slightly lower than the borates. Cr(III) emission could not be detected in the fluorozirconate glass.

Because of the low efficiencies, the $\bar{\tau}$ values listed in Table II (and defined in Sec. III B) can be interpreted as average $^4T_2 \rightarrow {}^4A_2$ radiationless decay rates. In general, the correlation between $\bar{\tau}$ and ϕ among these glasses is poor. This is especially true for the three fluorophosphate glasses which have closely similar $\bar{\tau}$ values yet vary by a factor of 4 in ϕ values.

D. Concentration quenching

It was shown in the previous section that integrating sphere measurements are not appropriate for investigating the effects of Cr(III)–Cr(III) interactions on quantum efficiency. This is because of the difficulty in accurately assessing the self-absorption error at high doping levels. For this reason lifetime measurements were used to measure the relative $^4T_2 \rightarrow {}^4A_2$ quantum efficiency as a function of Cr(III) concentration. In general, the Cr(III) emission decay accelerates as the Cr(III) concentration increases, so that $\bar{\tau}$ becomes smaller. Rather than use $\bar{\tau}$ to monitor relative quantum efficiency vs Cr(III) concentration curves, it was found that higher precision could be achieved by numerically integrating the experimental decay curve and using this area as a measure of relative ϕ. This measurement is proportional to total light intensity and is independent of any particular model of the nonexponential decay.

In Fig. 8 the data are summarized for soda lime silicate, aluminum phosphate, fluorophosphate, and lithium aluminum borate glasses. The features for each of these curves are similar. Below 0.01 mol% Cr(III), a plateau region is found in which the relative ϕ is independent of Cr(III) content. Above 0.01 mol% quenching becomes apparent until at 0.1 mol% the ϕ has decreased to 65% to 75% of its low concentration limiting value. At still higher Cr(III) concentrations the quenching behavior of the glasses differ somewhat in that ϕ decreases more slowly in aluminum phosphate and fluorophosphate relative to soda lime silicate. Measurements in the lithium aluminum borate could be made only to 0.2 mol% Cr(III) because higher Cr(III) contents led to devitrification. In other glasses samples with Cr(III) contents up to 1 mol% and higher could be prepared although we did not systematically investigate the regime above 1 mol%. It is interesting to note that there may be a connection between the low solubility of Cr_2O_3 in borate glass and the fact that optical spectra of Cr(III) in borates show the greatest inhomogeneous broadening. Both observations could result from an inability of borate glass to form suitable, presumably octahedral, sites for Cr(III) whereas silicate and phosphate glasses do better in this regard.

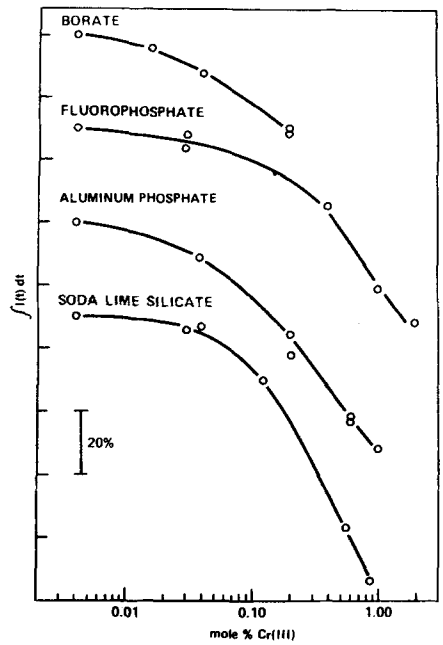

FIG. 8. Plots of the integrated experimental fluorescence decay for lithium aluminum borate, fluorophosphate 2, aluminum phosphate, and soda lime silicate glass are shown as a function of Cr(III) concentration. The areas measured for the lowest concentration glasses were set equal to unity and one division along the vertical axis represents a 20% reduction in area.

E. Hydroxyl quenching in silicate glass

A possible mechanism for radiationless relaxation of the Cr(III) $^4T_2$ state is quenching by hydroxyl groups which are invariably present in oxide glass. The quenching should occur because the third harmonic of the hydroxyl stretching fundamental at 3500 cm^{-1} provides a fair energy match to the Cr(III) fluorescence. Since a

TABLE IV. Optical parameters for dried silicate glasses.

Glass	$A(2.8\mu)$[a]	Fraction O atoms present as hydroxyl	$\bar{\tau}$ (μs)	ϕ[b]
Soda lime silicate	0.045	4.0×10^{-5}	27	0.06
Soda lime silicate	0.090	8.0×10^{-5}	27	0.05
Soda lime silicate	0.15	13.2×10^{-5}	29	0.06
Lithium lime silicate	0.23	20.4×10^{-5}	37	0.11

[a]Absorbance ($\log_{10} I_0/I$) of 0.2 cm thick samples measured at 2.8 μ. These values were converted to absolute hydroxyl concentrations using the extinction coefficient 77.5 1 mol^{-1} cm^{-1} after Ref. 46.
[b]These are measured quantum yields uncorrected for concentration quenching and self-absorption effects. The Cr(III) content of the soda lime silicates was 0.1 mol% and for the lithium lime silicate it was 0.05 mol%.

high order process is involved, it is likely that the interaction will be significant over short distances and perhaps only when the hydroxyl oxygen is coordinated to Cr(III). The fraction of oxygen atoms present as hydroxyl was established by measuring the infrared absorption at 2.8 μ which corresponds to the OH stretching fundamental. In a typical silicate glass, we find that 10^{-4} of the total oxygen content is present as hydroxyl. At this low level it seemed likely that OH plays no significant role in $^4T_2$ relaxation. Nevertheless, a series of silicate glasses were prepared in which the hydroxyl content was varied by a factor of four by drying procedures. Among this series there was no correlation between either $\bar{\tau}$ or ϕ and the OH content (see Table IV), so we conclude that OH does not affect the $^4T_2$ relaxation in silicates. Since the OH level of the other glasses were at comparably low levels, we assume the same is true in these hosts.

IV. DISCUSSION

The two principal results of this investigation are that for the majority of Cr(III) sites in a wide variety of glasses the zero phonon $^4T_2$ level lies lower than the zero phonon ^2E, i.e., the sites are low field, and that fluorescence from these sites is inefficient. As pointed out by others,[17] it is easy to understand in a qualitative sense why oxide and fluoride glasses are predominantly low field hosts. First, oxygen and fluorine lie low in the spectrochemical series.[30] This series is an empirical ordering of the magnitude of ligand fields produced by coordinated ions and crudely reflects the ligand ionic radius. A larger ionic radius should result in a smaller ligand field simply because the ligand electrostatic field is diminished. Second, because of their lack of long range periodicity, glasses tend to form open, low density structures which result in large Cr–ligand distances. It is known that in octahedral coordination, D_q is inversely proportional to the fifth power of this distance.[31] Third, many coordinated oxygens are covalently bonded to network forming ions which bear a high formal charge such as B^{3+}, Si^{4+}, and P^{5+}. These highly charged ions will sharply reduce the electron charge density available for coordination to Cr(III) and thereby reduce the ligand field. For all of these reasons it is not unexpected that glasses tend to be low field hosts. What is less obvious is why Cr(III) fluoresces inefficiently in glass sites.

The absolute quantum efficiency of $^4T_2 \rightarrow {}^4A_2$ fluorescence is 0.1 for most of the glasses studied here. The lithium lime silicate is somewhat anomalous with $\phi = 0.17$, but even in this case the $^4T_2$ relaxation is primarily nonradiative. Three possible mechanisms were investigated to explain these low efficiencies: multiphonon relaxation as applied to rare earth impurity centers, concentration quenching, and quenching by hydroxyl groups.

The relaxation of trivalent rare earths in solids by multiphonon emission is a theoretically well-founded and an experimentally well-documented phenomenon.[32] In principle, only two parameters are required to calculate the relaxation rate between levels, the energy gap to be bridged ΔE and the phonon cutoff energy of the host ω_0. This picture is frequently complicated by the presence of multiplets so that a Boltzmann distribution among initially populated levels and simultaneous relaxation to a multiplet of final levels must actually be considered. Nevertheless, clear criteria exist for establishing the efficacy of this mechanism in solids. The fluorescence maxima of the glasses listed in Table III all lie in the range $11\,700 \pm 650$ cm^{-1}. If it is assumed that the $^4T_2$ zero phonon levels parallel the band maxima, then a comparably small energy spread of $^4T_2$ levels exists among these glasses. This implies that if multiphonon emission to host lattice phonon modes is the relaxation mechanism, then the dominant factor causing differences in rate among glasses must be the host phonon cutoff energy, since ΔE is similar in all cases. An inspection of Table III shows that there is, in fact, no correlation between ω_0 of the glasses and radiative efficiency. The worst hosts for fluorescence, apart from the fluorozirconate which shows no emission, are the borates, the tellurite, and the phosphotungstate. These glasses are at opposite limits in the available range of host ω_0 values and should show the largest disparity in quantum yields with tellurite and phosphotungstate being the best hosts and borate being the worst. Instead, they have equally poor efficiencies with $\phi = 0.01$. On the other hand, those glasses with intermediate ω_0 energies, the silicates and the phosphates, have in some cases efficiencies higher by an order of magnitude or more. It seems clear that the multiphonon model as applied to rare earths cannot explain the Cr(III) $^4T_2$ results. It should be mentioned that the theory derived for relaxation of rare earth multiplets

TABLE V. Summary of $^4T_2$ lifetimes in crystalline hosts.

Crystal	τ^a (μs)	Cr(III) site symmetry	Reference
TiO_2	45	D_{2h}	2
MgO	35	Rhombic	8
$ZnWO_4$	10	Rhombic	4
$LiTaO_3$	10	C_3	3
$LiNbO_3$	11	C_3	3
K_2NaGaF_6	620	O_h	5

[a]All measurements made at liquid He temperature except for MgO which was at 77 °K.

was explicitly designed for the weak electron-phonon coupling limit and cannot necessarily be expected to adequately treat the dynamics of the $^4T_2$ level since it is obvious from the optical spectra that this level is in another coupling regime. However, it would not have been prudent to discount *a priori* the traditional relaxation mechanism without experimental verification.

Concentration quenching was also considered as a possible explanation for the low efficiency in glass, and Fig. 8 summarizes the relative efficiency data as a function of Cr(III) content for four glasses. Since the Cr(III) doping level of the samples used for integration sphere measurements was 0.02 mol% Cr_2O_3, Fig. 8 shows that the loss of efficiency due to Cr(III)–Cr(III) interaction was minor and the ϕ values could easily be corrected for the effect. The origin of the loss at high Cr(III) levels is not known at present. Fournier *et al.*,[33] in an electron spin resonance study of Cr(III) doped phosphate glass, showed that chromium pairs are a major constituent at high doping levels, and it seems likely that such a species could serve as an energy trap. In all cases, the fluorescence lifetime shortens with increasing Cr(III) content so that formally the trap concentration depends on Cr(III). It is also true that transition metal phase segregation can occur at high doping levels[34] which would lead to Cr(III) density fluctuations and presumably enhance the quenching. Indeed, Brawer and White[18] found their silicate glass to be spacially inhomogeneous, since the Cr(III) fluorescence spectrum was dependent on the position of the sample in the excitation beam. This could be a result of phase segregation. Spectra of our glasses were acquired at a doping level (0.02 mol% Cr_2O_3) a factor of ten less than Brawer and White[18] to avoid self-absorption artifacts, and spacial inhomogeneities were not evident.

At this point it is instructive to consider what is known about the Cr(III) $^4T_2 \rightarrow {}^4A_2$ radiative efficiency in crystalline hosts. Although no direct measure of efficiency has been previously reported for any low field material, it has frequently been assumed on the basis of circumstantial evidence that this transition is largely radiative. In Table V are listed in the $^4T_2$ lifetimes measured at liquid He or N_2 temperature for a number of low field hosts and the data appear to cast some doubt on this assumption. It is shown in Table V that the value for τ is similar for all materials in which the Cr(III) site symmetry is low. These τ values are not very different from typical glass $\bar{\tau}$ values also measured at low temperature. The notable exception in Table V is K_2NaGaF_6 in which the Cr(III) $^4T_2$ lifetime is 620 μs. This is the one host which is known to provide a rigorously O_h site symmetry. *Provided* the $^4T_2$ radiative lifetime is similar in all these hosts, these results suggest that there is a correlation between site symmetry and $^4T_2$ fluorescence efficiency, and that a symmetry selection rule may exist for the radiationless transition. If this is the case, then there is a clear rationale for explaining the low fluorescence efficiencies in glass. The disorder in a glass host coupled with the fact that coordinated ligands can be bound to network modifying or network forming cations insures that the Cr(III) sites in glass are not O_h. Presumably, then, the prohibition for nonradiative relaxation is not operative and the efficiencies can be low. It is important to realize that this result should apply to all possible glass formulations, since by the very nature of this disordered state a major improvement in symmetry cannot be anticipated. The theoretical basis for an electronic symmetry selection rule in radiationless transitions has been known for a number of years.[35,36] The rate for a radiationless process between Born–Oppenheimer states driven by the nonadiabatic operator is formally given by the following summations:

$$W(i \rightarrow f) = 2\pi \sum_{v'v''} P_{v'} \sum_s R_s(f,i)^2 \left| \langle X_{fv''_s} \right| \frac{\partial}{\partial Q_s} \left| X_{iv'_s} \right\rangle \right|^2 \times \prod_{j \neq s} \left| \langle \chi_{fv''_j} | X_{iv'_j} \rangle \right|^2 \delta(E_{fv''} - E_{iv'}) ,$$

where

$$R_s(f,i) = -\hbar^2 \langle \phi_f | \frac{\partial}{\partial Q_s} | \phi_i \rangle . \quad (8)$$

In this expression for $W(i \rightarrow f)$, $X_{iv'}$ and $X_{fv''}$ are the initial and final vibrational wave functions, P_v are partition functions which give the Boltzmann population distribution among initial states, and $R_w(i,f)$ is an electronic factor which contains the selection rule.[37] In order for the electronic integral to be nonvanishing Q_s must be of proper symmetry to mix ϕ_f and ϕ_i. It has been pointed out by us,[38] and earlier by others,[39,40] that in the particular case of $^4T_{2g} \rightarrow {}^4A_{2g}$ relaxation, Q_s must be t_{1g}. This normal mode is absent in a seven atom octahedral complex, so that $w(i \rightarrow f)$ must vanish identically and relaxation between T_{2g} and A_{2g} states can only be radiative. This analysis, however, is too simplistic in several respects. One need only consider the next nearest neighbors in a solid to generate a normal mode of the required t_{1g} symmetry, and it is not known how strongly the $^4T_{2g}$ state is coupled to this more remote nuclear motion. Also, the $^4T_{2g}$ will undergo Jahn–Teller distortion prior to attaining the relaxed, luminescent configuration, and so the relevant state symmetry will be lowered although inversion will be retained. It seems apparent that a detailed theoretical analysis is required to assess these points; however, the data available to date suggest that the simple vibrational deficiency model may be close to reality.

Although it is certain that the Cr(III) $^4T_2$ level is not well described as a weak phonon coupling case, it is not certain whether it lies in the strong coupling limit as typi-

fied by alkali halide F centers. Nevertheless, it is useful to briefly consider radiationless relaxation in this limit since it is well understood and may be an appropriate model for the $^4T_2$ state. The factors governing F center radiative efficiency are defined in terms of the relative positions of ground and excited state adiabatic potential surfaces. Bartram and Stoneham[41] have shown that three parameters obtainable from optical spectra enable an accurate prediction to be made about luminescence efficiency. These are the transition energy of the optical absorption E, the mean number of phonons created in the vertical transition S (the Huang–Rhys factor), and the phonon energy E_{phonon}. A criterion has been formulated such that $\Lambda = SE_{\text{phonon}}/E \leq 0.25$ in order for luminescence to occur. This criterion is a consequence of Dexter, Klick, and Russell's[42] original proposal that F center luminescence is possible only when the energy of the vertical transition E is less than the energy at the crossing point of ground and excited state potential surfaces. If the excitation energy exceeds the crossing energy ($\Lambda > 0.25$), then the system relaxes by phonon emission via the crossing and thermally equilibrated excited state is never achieved. If the excitation energy is less than the crossing energy ($S < 0.25$), then the system luminescence with high efficiency. Unfortunately there is a near total lack of detailed spectroscopic data needed to test Bartram and Stoneham's[40] criterion for the Cr(III) $^4T_2$ state. An analysis by Wilson and Solomon[43] of this state in the molecular complex $Cr(NH_3)_3$ has appeared recently. Using their parameters, $\Lambda = 5 \times 403\ \text{cm}^{-1}/22\,300\ \text{cm}^{-1} = 0.09$, well within Bartram and Stoneham's criterion of 0.25 for strong luminescence. However, this complex does not fluoresce and for a good reason, it is a high field case and the $^4T_2$ radiationless decay to ^2E completely precludes $^4T_2$ emission. The $^4T_2$ lifetime is known to be subnanosecond in other high field materials because of this relaxation.[44]

One intuitively feels that Cr(III) $^4T_2$ in a low field host will also satisfy the $\Lambda \leq 0.25$ requirement because the optical spectra in the two limits are quite similar, but no analysis of a low field case has appeared. Glasses are not good candidates for such detailed analysis because of inevitable error due to inhomogeneous broadening and a complete lack of vibronic structure even at liquid He temperature. This latter drawback could, in principle, be overcome, as it is in the case of F centers by temperature dependent studies; but apparently large errors can accrue due to the forbidden nature of the transition.[45] Clearly, a need exists for detailed spectroscopic and photokinetic studies of low field crystalline hosts to unravel detail of the nonradiative process. From the limited data presently available, it seems likely that such studies will reveal that the $^4T_2$ lies in some intermediate electron–phonon coupling regime and that the factors of importance in determining its relaxation dynamics will be different than those operative in the strong and weak coupling limits.

ACKNOWLEDGMENTS

Partial support for this work from the Office of Advanced Energy Concepts, Department of Energy under contract ER-78-C-02-4996 A000 is gratefully acknowledged. Special thanks are due to Diane Guenther for her skill and careful attention to detail in the glass preparations. We also wish to thank Professor E. I. Solomon of MIT for making the low temperature absorption spectrometer available to us, Mr. G. Spears of GTE Sylvania Danvers Lighting Center for providing the calibrated working standard lamps, and to Dr. M. Weber of Lawrence Livermore Laboratories for supplying the lithium lime silicate 2 and fluorozirconate glasses.

[1] D. L. Wood, J. Ferguson, K. Knox, and J. F. Dillon, Jr., J. Chem. Phys. **39**, 890 (1963).
[2] L. Grabner, S. E. Stokowski, and W. S. Brower, Jr., Phys. Rev. B **2**, 590 (1970).
[3] A. M. Glass, J. Chem. Phys. **50**, 1501 (1969).
[4] M. L. Reynolds, W. E. Hagston, and G. F. J Garlick, Phys. Status Solidi **30**, 113 (1968).
[5] J. Ferguson, H. J. Guggenheim, and D. L. Wood, J. Chem. Phys. **54**, 504 (1971).
[6] R. W. Schwartz, Inorg. Chem. **11**, 2817 (1976).
[7] H. U. Güdel and T. R. Snellgrove, Inorg. Chem. **17**, 1617 (1978).
[8] F. Castelli and L. S. Forster, Phys. Rev. B **11**, 920 (1975).
[9] M. O. Henry, J. P. Larkin, and G. F. Imbusch, Phys. Rev. B **13**, 1893 (1976).
[10] H. L. Schläfer, H. Gausmann, and H. Witzke, J. Chem. Phys. **46**, 1423 (1967).
[11] H. L. Schläfer, H. Gausmann, and H-U. Zaner, Inorg. Chem. **6**, 1528 (1967).
[12] G. B. Porter and H. L. Schläfer, Zeit. Phys. Chem. **37**, 109 (1963).
[13] A. D. Kirk and G. B. Porter, J. Phys. Chem. **84**, 887 (1980).
[14] J. H. Parker, Jr., R. W. Weinert, and J. G. Castle, Jr., in *Optical Properties of Ions in Crystals*, edited by H. M. Crosswhite and H. W. Moos, Interscience, New York, 1967), p. 251.
[15] C. R. Bamford, Phys. Chem. Glasses **3**, 189 (1962).
[16] T. Bates, in *Modern Aspects of the Vitreous State*, edited by J. D. MacKenzie (Butterworths, Washington, 1960), Vol. 2, Chap. 5.
[17] R. E. Tischer, J. Chem. Phys. **48**, 4291 (1968).
[18] S. A. Brawer and W. B. White, J. Chem. Phys. **67**, 2043 (1977).
[19] A. L. Lempicki, L. Andrews, S. Nettle, B. McCollum, and E. I. Solomon, Phys. Rev. Lett. **44**, 1234 (1980).
[20] G. O. Karapetyan, V. P. Kovalyov, and S. G. Lunter, Opt. Spectrosc. **19**, 529 (1965).
[21] E. J. Sharp, J. E. Miller, and M. J. Weber, Phys. Lett. A **30**, 142 (1969).
[22] M. J. Weber, E. J. Sharp, and J. E. Miller, J. Phys. Chem. Solids **32**, 2275 (1971).
[23] E. J. Sharp, J. E. Miller, and M. J. Weber, J. Appl. Phys. **44**, 4098 (1973).
[24] P. Nath, A. Paul, and R. W. Douglas, Phys. Chem. Glasses **6**, 203 (1965).
[25] M. D. Sturge, H. J. Guggenheim, and M. H. L. Pryce, Phys. Rev. B **2**, 2459 (1970).
[26] Y. Tanabe and S. Sugano, J. Phys. Soc. Jpn. **9**, 753, 766 (1954).
[27] L. S. Forster and R. Livingston, J. Chem. Phys. **20**, 1315 (1952).
[28] E. B. Rosa and A. H. Taylor, Natl. Bur. Stand. Sci. Paper 447 (1922).
[29] F. Grum and G. W. Luckey, App. Opt. **7**, 2289 (1965).
[30] C. K. Jorgensen, *Absorption Spectra and Chemical Bonding in Complexes* (Pergamon, Oxford, 1962), Chap. 7.
[31] F. E. Ilse and H. Hartmann, Z. Phys. Chem. **197**, 239

(1951).
[32]L. A. Riseberg and M. J. Weber, in *Progress in Optics*, edited by E. Wolf (North-Holland, Amsterdam, 1976), Vol. 14, p. 89.
[33]J. T. Fournier, R. J. Landry, and R. H. Bartram, J. Chem. Phys. **55**, 2522 (1971).
[34]P. W. McMillan, *Glass Ceramics* (Academic, New York, 1964), pp. 69–70.
[35]S. H. Lin, J. Chem. Phys. **44**, 3759 (1966).
[36]M. Bixon and J. Jortner, J. Chem. Phys. **48**, 715 (1968).
[37]F. Auzel, in *Luminescence of Inorganic Solids*, edited by B. DiBartolo (Plenum, New York, 1978), p. 67.
[38]L. J. Andrews, A. Lempicki, and B. C. McCollum, Chem. Phys. Lett. **74**, 404 (1980).
[39]P. J. Gardner and M. Kasha, J. Chem. Phys. **50**, 1543 (1969).
[40]D. J. Robbins and M. J. Thomson, Mol. Phys. **25**, 1103 (1973); Philos. Mag. **36**, 999 (1977).
[41]R. H. Bartram and A. M. Stoneham, Solid State Comm. **17**, 1593 (1975); Solid-State Elect. **21**, 1325 (1978).
[42]D. L. Dexter, C. C. Klick, and G. A. Russell, Phys. Rev. **100**, 603 (1955).
[43]R. B. Wilson and E. I. Solomon, Inorg. Chem. **17**, 1729 (1978).
[44]P. N. Everett, J. Appl. Phys. **41**, 3193 (1970).
[45]E. I. Solomon (private communication).
[46]G. Hetherington and K. H. Jack, Phys. Chem. Glasses **3**, 129 (1962).